KSCE Journal of Civil Engineering (2020) 24(1):219-227
DOI 10.1007/s12205-020-0588-y

pISSN 1226-7988, eISSN 1976-3808
www.springer.com/12205

Structural Engineering

Experimental Study on Thermal Conductivity of Concrete Using Ferronickel Slag Powder

Chang-Hong Lee[a], **Sang-Chel Kim**[b], **Young-Jin Kim**[c], **Seong-Kyum Kim**[d], **Jun-Pil Hwang**[e], **and Joon-Woo Park**[f]

[a]*Material & Structure Research Group, POSCO E&C, Incheon 22009, Korea*
[b]*Dept. of Civil Engineering, Hanseo University, Seosan 31962, Korea*
[c]*Member, Engineering Research Center, Korea Concrete Institute, Seoul 06130, Korea*
[d]*Member, Dept. of Civil Engineering, Kumoh National Institute of Technology, Gumi 39177, Korea*
[e]*Member, CMME, Seoul 04166, Korea*
[f]*Member, Track & Roadbed Research Team, Korea Railroad Research Institute, Uiwang 16105, Korea*

ARTICLE HISTORY

Received 22 April 2019
Revised 1st 30 Junuary 2019
Revised 2nd 1 October 2019
Accepted 24 October 2019
Published Online 2 December 2019

KEYWORDS

Ferronickel slag (FNS)
Thermal conductivity
Compressive strength
Pore structure
Concrete

ABSTRACT

Insulation performance of concrete must be secured in order to minimize the energy loss of buildings. For enhancing the insulation performance of concrete, this study conducts research on thermal conductivity of concrete using the Eco-friendly material called ferronickel slag (FNS) binder, and compares the mechanical properties and insulation properties to the concrete using ordinary Portland cement (OPC). According to the tests results, the compressive strength of 91days 100%OPC and 30%FNS concrete were 36.4 and 36.3 MPa, respectively. Given that the activity of FNS is almost equal to the 100%OPC at the long-term curing period, it appears that the unhydrates and pore water from the secondary hydration reaction have negligible influence on the mechanical property of concrete. The test result also shows that 91days 100%OPC and 30%FNS concrete have insulation performance of 1.59 and 1.10W/mK, respectively, indicating that thermal conductivity of FNS is 31% lower than that of OPC. The lower thermal conductivity of FNS appears to be caused by uniform heat transfer resulted from the presence of unhydrates, surplus water, and pores, at the level of avoiding degradation the structural performance. Therefore, it is concluded that insulation performance of concrete is improved by the use of FNS.

1. Introduction

Interest in energy usage continues to grow due to the recent rapid change in the climate environment caused by the greenhouse gas emission. Since buildings account for 40% of the Organization for Economic Cooperation and Development (OECD) national energy use, it is considered to be an important task to reduce the energy consumption by improving the insulation property of buildings (UNEP, 2008). Concrete is widely used as the interior and exterior materials for buildings, because it comprises about 70% of the building envelope and it has the low thermal conductivity which is only about 1/40 – 1/50 of the construction materials such as steel (Spicer et al., 1998). Concrete is a complex construction material consisted of various elements such as air, coarse aggregates, fine aggregates, and hydrates, with the insulation performance that is closely related to the thermal conductivity. Insulation performance can be improved by adjusting internal pores, materials, and mix designs. Research findings points out that thermal conductivity can be decreased by securing the isolated pores and internal pores using porous lightweight aggregate and diatomite powder (Mindess et al., 2003; Khalil et al., 2005; Aydin and Gul, 2007; Munch, 2009). Other researches also suggest that the insulation performance of concrete can be improved by using Eco-friendly porous materials such as porous hydrated lime and porous activated carbon (Wang and Shih, 2005; Cheeseman and Virdi, 2005). Thus far, researches have focused on non-structural concretes, and have indicated that it is difficult to earn workability among the properties of fresh

CORRESPONDENCE Joon-Woo Park jwp11188@krri.re.kr Track & Roadbed Research Team, Korea Railroad Research Institute, Uiwang 16105, Korea

ⓒ 2020 Korean Society of Civil Engineers

concrete, by using the abovementioned materials. Therefore, it is necessary to ensure the insulation performance in the concrete that comprises the building envelope, and also to pursue further studies regarding the structural concrete with improved insulation performance.

This study conducts research regarding the improved thermal conductivity of concrete using the Eco-friendly material called Ferronickel Slag (FNS) powder, in order to enhance the insulation performance of concrete. FNS is a useful by-product of the Ferronickel production which is obtained by melting the raw materials at high temperature and separating Ferronickel. Nations such as Greece, China, Australia, Japan, and Korea have long been using the FNS in various ways (Lee, 2017; Lee et al., 2018). FNS has mostly been utilized as aggregates in researches. Only since 2015, initial stage of research began regarding the hydration reaction and mechanical properties of FNS. FNS is bound in crystalline structure known as forsterite (Mg_2SiO_4), and its major oxides are SiO_2, MgO, Fe_2O_3, CaO, Al_2O_3. The quality of the slag varies depending on the manufacture even if they are based on the same production purpose of Ferronickel (Yang and Zhang, 2014; Choi and Choi, 2015). Therefore, high-alumina FNS and Blast furnace FNS display the property of rapid hardening, according to the chemical component and cooling method of the raw materials (Dourdounisa et al., 2004). Electric arc FNS display no hydration reactivity. When mixed with ordinary Portland cement (OPC), it reacts with $Ca(OH)_2$ to create C-S-H gel, thereby contributing to the long-term strength enhancement (Lemonis et al., 2015). Researches have compared the performance of FNS with other representative cement substitutes called ground granulated blast furnace slag (GGBS) and pulverised fuel ash (PFA). GGBS had higher hydration heat and reactivity compared to FNS. Compressive strength and chloride ion penetration resistance decreases when using FNS (Huang et al., 2017). On the other hand, FNS mixed mortar had similar compression strength compared to the strength of PFA (Rahman et al., 2017; Cho et al., 2018). Currently the technological development paradigm of FNS is progressing in the following order: bank materials/roadbed materials -> aggregate substitutes -> cement replacement substitutes. However, it still remains at the initial stage with sufficient fields of further technological development.

In this study, insulation performance is compared between 100%OPC and substituted FNS concrete, through the cement matrix thermal conductivity test and pore structure analysis. Particularity regarding the thermal conductivity enhancement, the study investigated the pore structure properties of concrete substituted with FNS by using mercury intrusion porosimetry (MIP) and image analysis techniques. In addition, it examined the effect of pore structure on the insulation performance and mechanical properties.

2. Experiments

2.1 Materials and Specimens

This study used OPC and FNS as the binder of producing paste, mortar and concrete. Major chemical compositions and material properties are presented in Table 1. OPC type I was used and FNS, a product of Korean company "S" used, was produced by pulverizing the prime sand that was obtained from spraying water into the molten slag for rapid cooling. The thermal conductivity can be greatly affected by the shape, density, and porosity of the aggregate. Therefore, appropriate aggregates conforming to the standard were used to minimize the impact of aggregate caused by the mix proportion. For fine aggregates, washed aggregate with specific gravity of 2.60 g/cm^3 and fineness modulus of 2.73 is used. For coarse aggregates, crushed aggregate with specific gravity of 2.62g/cm^3 and maximum size of 25 mm is used. Two types of concrete mix design for compression strength test and thermal conductivity test are shown in Table 2. Both 100% OPC and 30% FNS are performed

Table 1. Chemical Compositions and Material Properties of OPC and FNS

	Main oxide compound (%)						Ignition loss (%)	Fineness (cm^2/g)	Specific gravity (g/cm^3)
	CaO	MgO	Al_2O_3	SiO_2	Fe_2O_3	SO_3			
OPC	66.9	1.6	3.9	17.4	4.1	3.4	2.4	3,712	3.12
FNS	0.6	27.4	2.2	51.0	15.5	0.1	-	4,666	3.05

Table 2. Mix Proportions of Cement Paste, Mortar, Concrete

Types		W/B	s/a	Unit weight of materials (kg/m^3)				
				Water	OPC	FNS	Fine aggregate	Coarse aggregate
Cement paste	100%OPC	0.467	-	595.3	1274.8	0.0	-	-
	30%FNS	0.467	-	595.3	892.3	382.4	-	-
Mortar	100%OPC	0.467	1.0	274.8	588.5	0.0	1432.0	-
	30%FNS	0.467	1.0	274.8	411.9	176.5	1432.0	-
Concrete	100%OPC	0.467	48.1	164.9	353.0	0.0	859.0	931.0
	30%FNS	0.467	48.1	164.9	247.1	105.9	859.0	931.0

Fig. 1. Set-Up of Conducting the Chamber Test: (a) Concrete Specimen, (b) Experiment Equipment

in accordance with the design compressive strength (f_{ck}) 35 MPa. In this study, W/B ratio and aggregate amount were controlled to study the void characteristics according to the binder type. In order to minimize the impact of aggregate, binder is replaced using volume ratio, and the same amount of aggregate is mixed. The mortar design mix for the pore structure analysis uses the same unit cement amount and W/B as the concrete mix, applying the binder: water: aggregate ratio of 1.00: 0.47: 2.43. Paste specimen is used to check the hydrates and to measure the pore volume. FNS was replaced according to volume ratio before use.

2.2 Thermal Conductivity

In this study, thermal conductivity test was performed in accordance with the flat plate comparison method, in order to assess the insulation performance of mortar and concrete. As a specimen, mortar is created at the size of 300 × 300 × 50 mm. For the testing equipment, thermal conductivity meter is used. The thermal conductivity meter consists of a high-temperature plate, a low-temperature plate, a standard plate, a high-temperature source, a low-temperature source, and a thermometer. Thermal conductivity measures the steady-state heat transfer, and the temperature is monitored until the surface temperature of standard plate and specimen remain same.

Once the surface temperatures of standard plate and specimen became steady, the temperatures were measured every 15 minutes until the temperatures changes no more than 1% within the 30 minutes interval. Thermal conductivity is calculated using the following formula.

$$Thermal\ conductivity(W/m \cdot k) = \frac{l}{R_c} \tag{1}$$

$$R_c = \frac{A \cdot (\theta_1 - \theta_2)}{P} \tag{2}$$

Where,

A = Cross sectional area (m^2)
l = Thickness of the specimen (m)
P = Thermal conductivity
R_c = Thermal resistance of the specimen (m^2·K/W)
θ_1 = Hot side temperature (K) (°C)
θ_2 = Low side temperature (K) (°C)

2.3 Chamber Test

In this study, chamber test was conducted to assess the heat transfer rate of the concrete at each temperature interval. The specimen and equipment are shown in Fig. 1. In order to measure the internal temperature of concrete according to the outdoor temperature variation, three high-temperature thermocouples are embedded in the middle of 100 × 100 × 400 mm specimen. Temperature of electric arc oven was set at 800°C for the chamber test. The temperature is set to rapidly increase until the internal temperature of the chamber reaches the targeted value. The internal temperature change of each specimen was monitored by the rapid change of temperature. Internal temperature of the concrete is monitored every 30seconds for an hour. Average value of three temperatures measured from three thermocouples is applied.

2.4 Compressive Strength

For the compressive strength measurement, the concrete specimen was manufactured using Φ100 × 200 mm cylinder mold, and the mortar specimen was manufactured using 50 × 50 × 50 mm cube mold. The specimens were cured at the thermo-hydrostat chamber with the condition of 20 ± 2°C, R.H. 95%. The compressive strength was measured according to the KS F 2405 (Standard test method for compressive strength of concrete) at 3, 7, 14, 28, 91days, considering the thermal conductivity test.

2.5 Pore Structure

For analysis of pore structure of cement paste, MIP test and backscattered electron (BSE) analysis were performed to investigate the thermal conductivity of mortar and concrete. A sample of approximately 10 mm^3 was taken from the mortar specimen to estimate the porosity and pore distribution. MIP (Autopore IV 9500, MICROMERITICS) was performed on the sample. Before measuring, the sample was dried for 2 days in order to completely remove the moisture inside the pore, at the

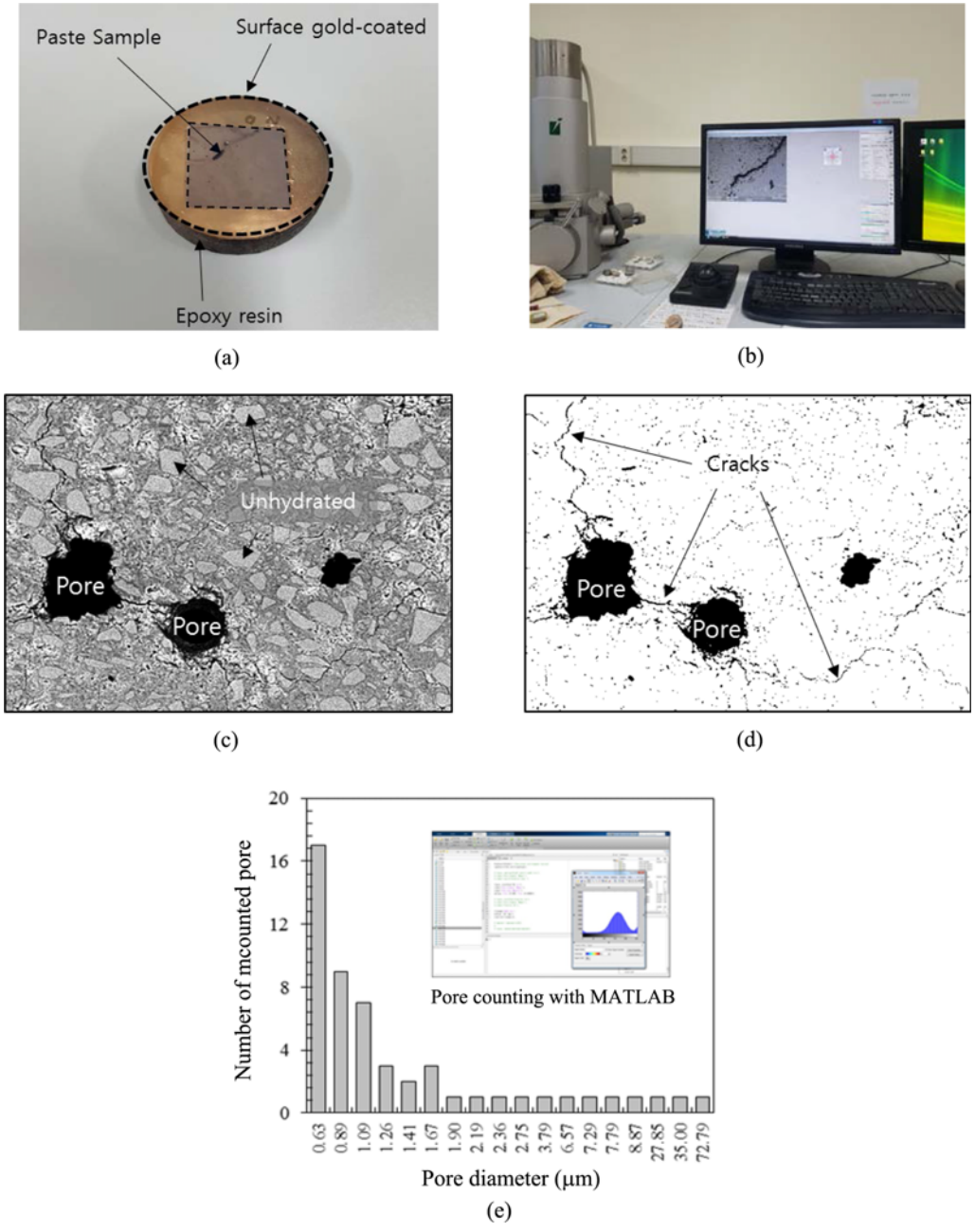

Fig. 2. Pretreatment of Samples for Porosity Quantification and Image Segmenting Sample, (b) Equipment, (c) Original Image, (d) Binary Image, (e) Pore Counting Using MATLAB

temperature of 50°C, which is the temperature interval that does not promote phase change.

2.6 SEM Image Analysis

A sample of approximately 10 mm^3 was taken from the mortar specimen to confirm the presence of entrained air. Based on the image from scanning electron microscope (SEM), qualitative analysis was performed regarding the ambient air of the aggregate. Epoxy resin was injected into the dried mortar to create the specimen, then the normal SEM was used to secure the image. On the secured original image and grayscale image, image segmentation was performed, The Microstructure analysis is shown in Fig. 2. Scanning electron microscope specifications used in this study were probe current 1pA-2nA, resolution 1.0 nm (15 kV), magnification x25-800,000, specimen size θ200 mm, and images were obtained by using Normal SEM to verify the pore distribution of mortar.

3. Results

3.1 Mechanical Property

The compressive strength test results of mortar and concrete are illustrated in Fig. 3. The compressive strength of 100%OPC mortar at the curing period of 3, 7, 14, 28, 91 days were 19.4,

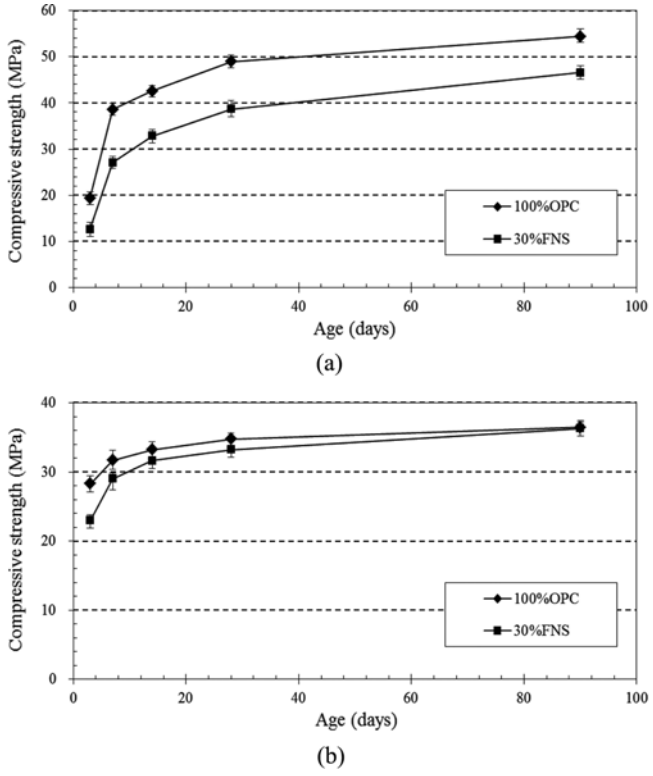

Fig. 3. Development of Compressive Strength of Mortar and Concrete with OPC and FNS: (a) Mortar, (b) Concrete

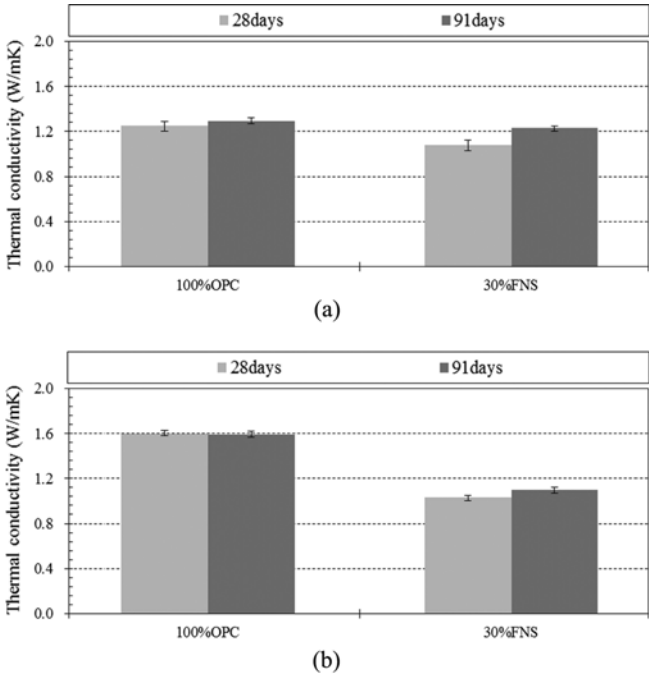

Fig. 4. Thermal Conductivity of the Mortar and Concrete with OPC and FNS: (a) Mortar, (b) Concrete

38.5, 42.5, 48.9, 54.4 MPa, respectively, indicating that the compressive strength of 100%OPC increases over curing time. The compressive strength of 30%FNS mortar at the curing period of 3, 7, 14, 28, 91 days were 12.7, 27.0, 32.8, 38.6, 46.6 MPa, respectively, indicating that the compressive strength of 30%FNS mortar increases over curing time. Compared to 100%OPC, the activity of 30%FNS mortar at the curing period of 3, 7, 14, 28, 91days were 65(± 1.5), 70(± 1.3), 77(± 1.4), 79(± 1.5), 86(± 1.4)%, respectively, indicating that the activity increases over curing time according to the secondary hydration reaction.

The compressive strength of 100%OPC concrete at the curing period of 3, 7, 14, 28, 91 days were 28.3, 31.7, 33.2, 34.8, 36.4 MPa, respectively, indicating that the compressive strength of 100% concrete increases over curing time. The compressive strength of 30% FNS concrete at the curing period of 3, 7, 14, 28, 91days were 23.0, 29.0, 31.6, 33.2, 36.3 MPa, respectively, indicating that the compressive strength increases of 30%FNS concrete as the curing age progresses. Compared to the 100%OPC, the activity of 30%FNS concrete at the curing period of 3, 7, 14, 28, 91 days were 81(± 1.1), 92(± 1.3), 95(± 1.0), 95(± 1.0), 100(± 1.1)%, respectively. At the curing period of 91days, the activity of 30%FNS was measured to be the same as activity of 100%OPC. In order to minimize the impact of aggregate on the compressive strength, FNS was replaced using volume ratio to ensure that the amount of aggregate mixture remains same. Therefore, it is concluded that the pore structure and hydrate are the major influence factors for the compressive strength, rather than the aggregate.

3.2 Behavior of Thermal Dynamics

The thermal conductivity test result of mortar and concrete are illustrated in Fig. 4. At the curing period of 28days, the thermal conductivity of the 100%OPC and 30%FNS mortar were 1.25, 1.08 W/m·K respectively, indicating that the thermal conductivity of FNS mortar was measured to be 14% lower than the thermal conductivity of 100%OPC mortar. At the curing period of 91days, the thermal conductivity of the 100%OPC and 30%FNS mortar were 1.29, 1.23 W/m·K respectively, indicating that the thermal conductivity of FNS mortar was measured to be 5% lower than the thermal conductivity of 100%OPC mortar.

At the curing period of 28days, the thermal conductivity of the 100%OPC and 30%FNS concrete were 1.60, 1.03W/m·K respectively, indicating that the thermal conductivity of FNS concrete was measured to be 36% lower than the thermal conductivity of 100%OPC concrete. At the curing period of 91 days, the thermal conductivity of the 100%OPC and 30%FNS concrete were 1.59, 1.10 W/m·K respectively, indicating that the thermal conductivity of FNS concrete was measured to be 31% lower than the thermal conductivity of 100%OPC concrete.

In the thermal conductivity test, equal aggregate ratio is applied to the cement matrix using OPC and FNS. The result indicates that use of 30%FNS results in lower thermal conductivity and improved insulation performance, compared to the use of 100%OPC. On the other hand, although same amount of W/B and cement was applied to mortar and concrete, the result revealed different value for thermal conductivity. Thermal

conductivity of concrete was measured to be higher than the mortar. It seems that the difference was caused by the effect of coarse aggregate, which is the biggest difference between mortar and concrete, along with the difference in volume ratio and porosity. The concrete coarse aggregate of concrete has high thermal conductivity (Davraz et al., 2015). In addition, thermal conductivity increases as the unhydrates and amount of pores decrease over the curing period. It appears that thermal conductivity increased with the hydration progression because unhydrates generally transfer heat rapidly due to its low density compared to other hydrates.

Both 100%OPC mortar and concrete display no significant change in the thermal conductivity at the curing period of 28 days and 91days. It appears that when using the FNS, secondary hydration reactions continues to occur during the mid-term and long-term curing period, thereby changing the cement matrix structure. In this regard, this study analyzed the pores on the cement matrix in relation to the porosity.

Change in internal temperature of the 28 days 100%OPC and 30%FNS concrete according to the external temperature change is illustrated in Fig. 5. As a result, 100%OPC concrete took 1,440 seconds to rise to 400°C whereas 30%FNS concrete took 1,600 seconds. For the internal temperature to rise to 800°C, 100%OPC concrete took 3,120 seconds whereas 30%FNS concrete took 3,450seconds. At the internal temperature of 400°C, the differential of 160 seconds exists between the time required by two types of concrete. At the internal temperature of 800°C, the differential of 330 seconds exists between the time required by two types of concrete. This result shows that the differential increases as the temperature increases, indicating that the heat transfer rate varies depending on the temperature interval. It can be suspected in Fig. 5 that the graph runs horizontally at the temperature of 20, 100, and 600°C. It appears that the graph trends reflect the active process of hydrates absorbing and decomposing the heat according to the temperature. Furthermore, it is plausible that the change in pore structure occurs at this time, which is the greatest influence factor on the thermal conductivity. Both 100%OPC and 30%FNS appears to have excellent insulation performance at low temperature intervals. Especially the internal temperature of the specimen reflected almost no change until the chamber temperature reaches 400°C. This is also related to the thickness of the specimen, but the thickness was not considered as a factor here since the experiment was intended to compare two types of mixture. Although other researchers (Mindess et al., 2003) have reported that the thermal conductivity of concrete aggregate has greatest impact on the thermal conductivity, the report could be considered unreliable since the volume and property of pores were not taken into consideration. In this study, same type and amount of aggregates were used in order to evaluate the thermal conductivity according to the volume and property of pores. Therefore, this study is expected to make contribution in grasping the volume and property of the pores as well as its impact. This is discussed in greater detail in the following section.

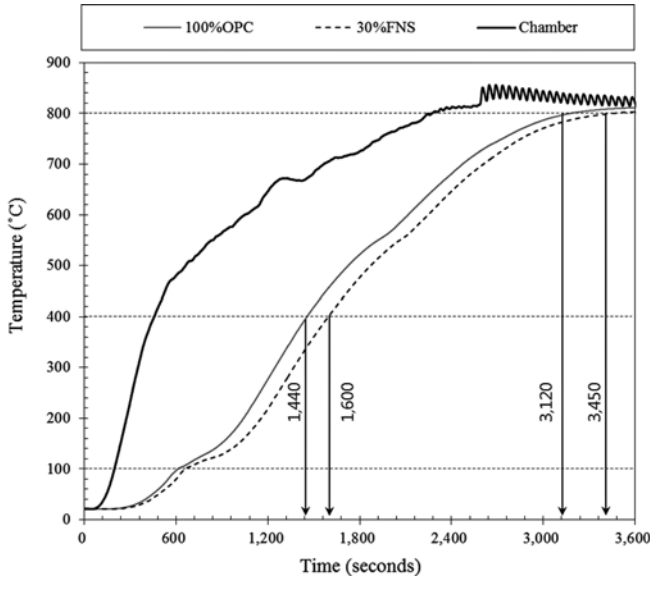

Fig. 5. Chamber Test Results of Concrete with OPC and FNS

3.3 Impact of Pore Structure

The MIP test results of 100% OPC paste are illustrated in Fig. 6.

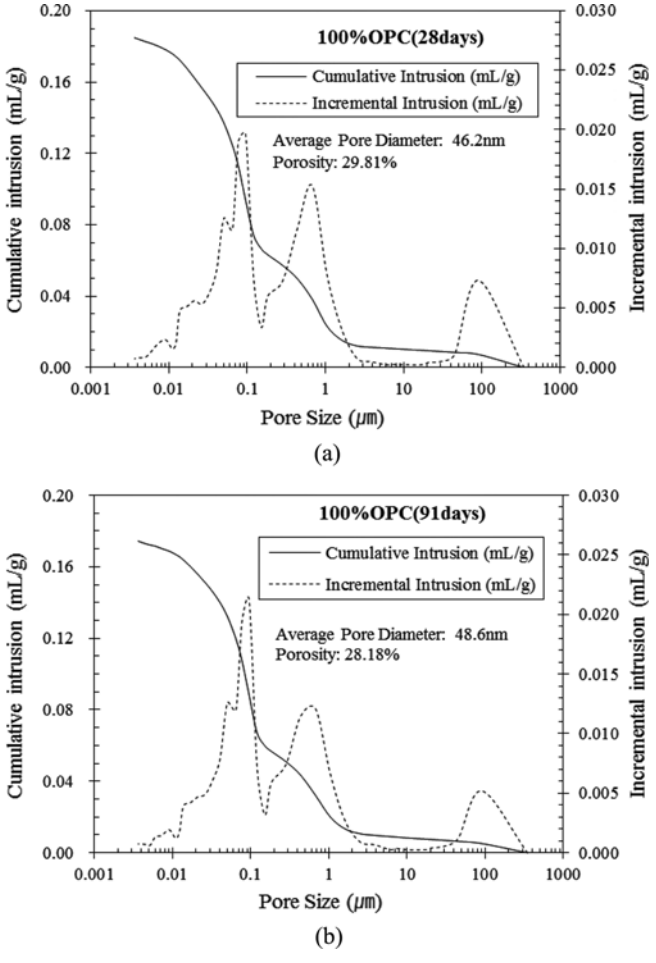

Fig. 6. Pore Size Distribution of 100%OPC Cement Paste: (a) 28 days, (b) 91 days

At the curing period of 28days and 91days, 100% OPC paste had porosity of 29.81% and 28.18%, respectively, and had the average pore diameter of 46.2 nm and 48.6 nm, respectively. Over curing time, the porosity decreased and the average pore diameter increased. It is plausible that change in porosity was caused by the hydration reaction as the Macro pores decrease while C-S-H gel is produced. Large pores with over 100 μm diameter are included in calculating the average pore diameter. It is suspected that the volume of Macro pores, which affects the mechanical property and durability of the cement matrix, increases over curing period.

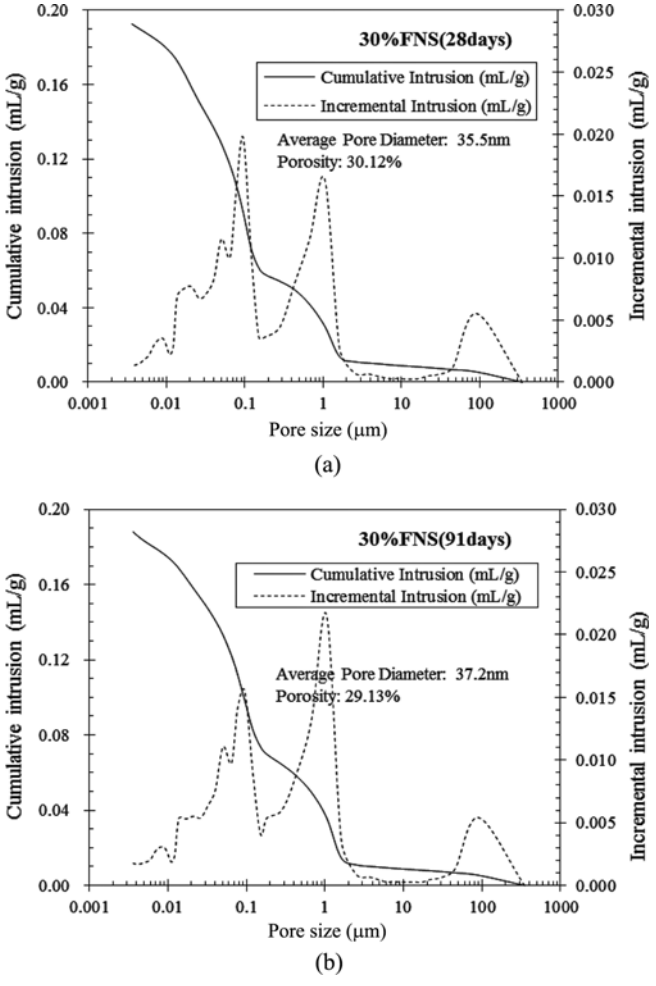

Fig. 7. Pore Size Distribution of 30%FNS Cement Paste: (a) 28 days (b) 91 days

The MIP test result of 30% FNS paste is illustrated in Fig. 7. At the curing period of 28 days and 90 days, 100%OPC paste had porosity of 30.12% and 29.13%, respectively, and had the average pore diameter of 35.5 nm and 37.2 nm, respectively. Over curing time, secondary hydration reaction of FNS creates C-S-H gel and Hydrotacite. As a result, Macro pores in between the secondary hydrates and $Ca(OH)_2$ decreases while micro gel pores increase, resulting in the overall porosity decrease. Therefore, it can be suspected that average pore diameter of 30%FNS paste display significant drop, compared to the 100%OPC.

According to the MIP result, second peak is formed regardless of the curing period at around 0.5 μm for 100%OPC and 1.0 μm for 30%FNS. In the case of 30%FNS, the second peak value increases and the first peak value decreases over time. This means that the average pore diameter became smaller and that the amount of C-S-H in OPC increased. In particular, the thermal conductivity is expected to increase because decreased average porosity helps to enhance the thermal conductivity.

Generally, the heat transfer rate is in the following order: solid > liquid > gas. There are various materials in the cement matrix such as crystaline hydrate, unhydrates (solid), C-S-H gel (liquid), and pores (gas). Image analysis is used to examine the effect of hydrates, unhydrates, and pore distribution on thermal conductivity. Heat transfer rate is fast in the case of homogeneous materials, and slow in the case of heterogeneous materials due to bypass transfer. The image of 100%OPC paste is illustrated in Fig. 8. It appears that OPC has small ratio of pores bigger than 100 μm because it has quick hydration reaction cauisng the low ratio of unhydrates and surplus water. It especially has low unhydrates, allowing the uniform heat transfer. Therefore, 100%OPC is expected to have fast heat transfer due to small ratio of pores over 100 μm and foreign materials.

The image analysis result of 30% FNS paste is illustrated in Fig. 9. The FNS replacement has slower hydration reaction compared to OPC that it has high ratio of unhydrates as well as the pores over 100 μm, large number of surplus water, and large

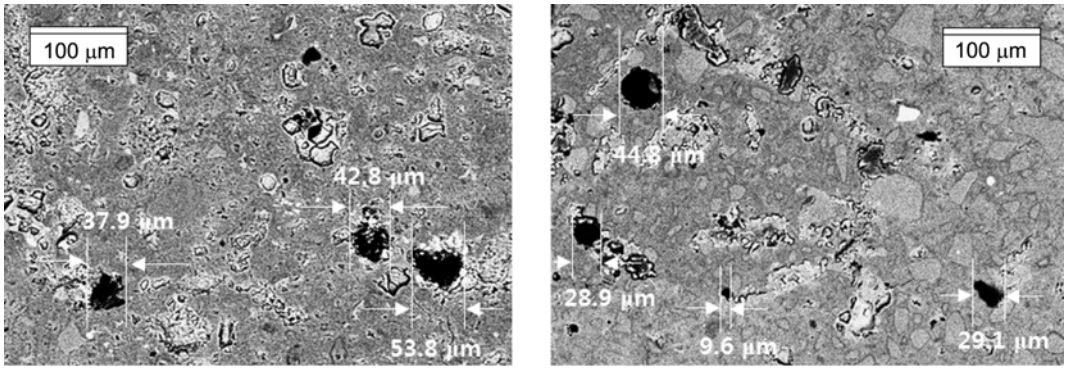

Fig. 8. Pore Structure of 100%OPC Cement Paste

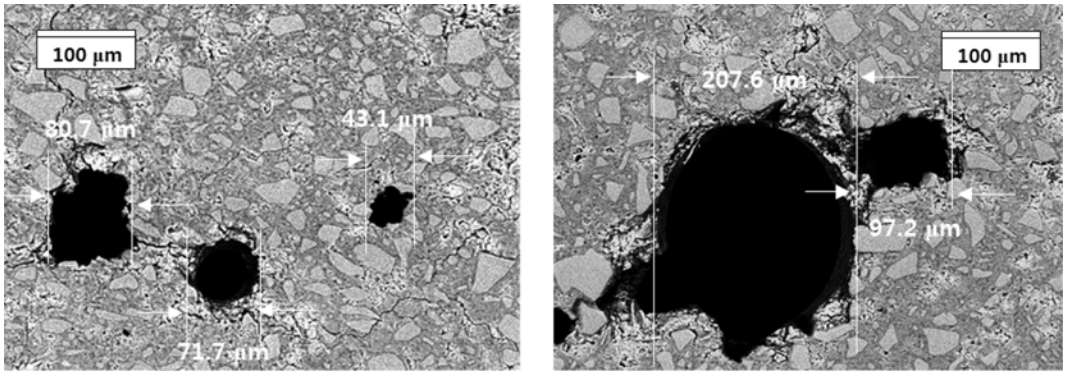

Fig. 9. Pore Structure of 30%FNS Cement Paste

Table 3. Pore Distribution Measurement Result

Types		Pore range (μm)						Total pore area (μm²)
		< 1	1 – 5	5 – 10	10 – 50	50 – 100	> 100	
100%OPC	Number of pores	2,044	1,894	163	82	15	0	1,1119.9
	Average pore diameter (μm)	0.76	3.44	7.09	13.61	55.96	0	
	Volume (%)	13.9	25.3	10.3	10.0	7.5	0	
30%FNS	Number of pores	689	693	71	57	3	7	5,877.0
	Average pore diameter (μm)	0.76	3.36	6.91	19.36	71.94	173.56	
	Volume (%)	8.9	39.6	8.3	18.8	3.7	20.7	

pore size. In particular, heat is not uniformly transferred because of the large amount of unhydrates. Therefore, it seems that 30%FNS has many pores over 100 μm, large pore size, and slow thermal conductivity. Therefore, it is concluded that the insulation performance of FNS is excellent since the thermal conductivity will decrease as the usage amount increases according to the material property and hydration mechanism.

BSE mode of SEM was used to take picture of the image, and MATLAB was used to turn the picture into binary image. Collected data was classified according to the pore size, and Table 3 offers the average pore size depending on the pore range. As a result, no pores over 100 μm was found in case of 100%OPC, whereas 7pores at the same size was found in 30%FNS. The average diameter of the pores found in 30%FNS was 173.59 μm which is considerably large pore size. On the other hand, large number of pores with short diameter was found in 100%OPC. In particular, there were about 2,044 pores with size that is smaller than 1 μm, which is about 3times more than the same size pores found in 30%FNS. Image analysis result indicates having large number of pores with large diameter is advantageous in heat transfer, whereas pores having small diameter has insignificant effect in heat transfer. The total area of the pores for 100%OPC was measured at 11,179.9 μm^2 whereas 30%FNS was measured at 5,877.0 μm^2. It seems that total area of the pores is irrelevant to the heat transfer. It is concluded that having large pores with the size over 100 μm in the matrix can enhance insulation performance by hindering heat transfer. Therefore, larger volume of the pores over 100 μm is required for the concrete with higher insulation performance.

The largest energy loss in the building is the shell of the structure, and research is being actively conducted to reduce energy loss in this area, but most of these studies are using windows and insulation. There is little research on concrete, which accounts for more than 70% of building envelopes. In addition to providing heat insulation performance to the concrete that forms the outer wall of the building, a new study on the improvement of heat insulation performance that can be used for structural purposes is newly required.

4. Conclusions

In this study, the thermal conductivity of mortar and concrete using 100%OPC and 30%FNS are investigated, and the conclusions are as follows:

1. The compressive test result reveals that compared to 100%OPC, the activity of 30%FNS concrete at the curing period of 28 days and 91days were 95% and 100%. It is concluded that use of FNS may affect the change in pore structure of cement matrix and hydrates as the secondary hydration reaction continues to progress.
2. The thermal conductivity test results show that 91days 30%FNS concrete had 31% lower thermal conductivity compared to 91 day 100%OPC concrete. It is concluded that the use of binder can improve the insulation performance of concrete.
3. According to the chamber test, 30%FNS took longer time

to increase the internal temperature of the concrete up to 800°C than 100%OPC. It is concluded that heat transfer rate varies depending on the temperature interval due to the change in hydrates caused by the use of FNS.

4. The result of pore structure test confirmed the presence of pores over 100 μm. It also suggests that the pores interfered with the heat transfer, thereby reducing the thermal conductivity of concrete. Therefore, it is concluded that insulation performance of concrete can effectively be improved by securing the pores over 100 μm at the level of not effecting the structure of concrete.

Acknowledgements

This research was supported by a grant from the Korea Concrete Institute (project number: KCI-R-18-009). The authors would like to thank in the support in finance.

ORCID

Chang-Hong Lee https://orcid.org/0000-0003-3639-8332
Sang-Chel Kim https://orcid.org/0000-0002-9149-8697
Young-Jin Kim https://orcid.org/0000-0003-1943-0994
Seong-Kyum Kim https://orcid.org/0000-0002-2014-8681
Jun-Pil Hwang https://orcid.org/0000-0002-5219-5837
Joon-Woo Park https://orcid.org/0000-0003-0262-9497

References

Aydin AC, Gul R (2007) Influence of volcanic originated natural materials as additives on the setting time and some mechanical properties of concrete. *Construction and Building Materials* 21(6): 1277-1281, DOI: 10.1016/j.conbuildmat.2006.02.011

Cheeseman CR, Virdi GS (2005) Properties and microstructure of lightweight aggregate produced from sintered sewage sludge ash. *Resources, Conservation and Recycling* 45(1):18-30, DOI: 10.1016/j.resconrec.2004.12.006

Cho BS, Kim YU, Kim DB, Choi SJ (2018) Effect of ferronickel slag powder on microhydration heat, flow, compressive strength, and drying shrinkage of mortar. *Advances in Civil Engineering* 2018:1-7, DOI: 10.1155/2018/6420238

Choi YC, Choi SC (2015) Alkali-silica reactivity of cementitious materials using ferronickel slag fine aggregates produced in different cooling conditions. *Construction and Building Materials* 99:279-287, DOI: 10.1016/j.conbuildmat.2015.09.039

Davraz M, Koru M, Akdag AE (2015) The effect of physical properties on thermal conductivity of lightweight aggregate. *Procedia Earth and Planetary Science* 15:85-92, DOI: 10.1016/j.proeps.2015.08.022

Dourdounisa E, Stivanakisa V, Angelopoulosa GN, Chaniotakisb E, Frogoudakisc E, Papanastasioud D, Papamantellosa DC (2004) High-alumina cement production from FeNi-ERF slag, limestone and diasporic bauxite. *Cement and Concrete Research* 34(6):941-947, DOI: 10.1016/j.cemconres.2003.11.004

Huang Y, Wang Q, Shi M (2017) Characteristics and reactivity of ferronickel slag powder. *Construction and Building Materials* 156:773-789, DOI: 10.1016/j.conbuildmat.2017.09.038

Khalil KMS, Elkabee LA, Murphy B (2005) Preparation and characterization of thermally stable porous ceria aggregates formed via a sol-gel process of ultrasonically dispersed cerium (IV) isopropoxide. *Microporous and Mesoporous Materials* 78(1):83-89, DOI: 10.1016/j.micromeso.2004.09.019

Lee CH (2017) The status of construction recycling resources in global ferronickel slag market. *Magazine of Korea Recycled Constriction Resources Institute* 12(3):54-58

Lee CH, Oh BJ, Kim SH, Kim JH (2018) In-situ application of concrete and pre-cast concrete structures using ferronickel slag powder. *Magazine of Korea Recycled Constriction Resources Institute* 13(1): 50-54, DOI: 10.14190/MRCR.2018.13.1.050

Lemonis N, Tsakiridis PE, Katsiotis NS, Antiohos S, Papageorgiou D, Katsiotis MS, Beazi-Katsioti M (2015) Hydration study of ternary blended cements containing ferronickel slag and natural pozzolan. *Construction and Building Materials* 81:130-139, DOI: 10.1016/j.conbuildmat.2015.02.046

Mindess S, Young JF, Darwin D (2003) Concrete, 2nd edition. Prentice Hall, Upper Saddle River, NJ, USA

Munch A (2009) Improving thermal insulation of concrete sandwich buildings. *Indoor and Built Environment* 18(5):424-431, DOI: 10.1177/1420326X09346139

Rahman MA, Sarker PK, Shaikh FUK, Saha AK (2017) Soundness and compressive strength of Portland cement blended with ground granulated ferronickel slag. *Construction and Building Materials* 140:194-202, DOI: 10.1016/j.conbuildmat.2017.02.023

Spicer JWM, Osiander R, Aamodt LC, Givens RB (1998) Microwave thermoreflectometry for detection of rebar corrosion. *Structural Materials Technology III: An NDT Conference* 402-409, DOI: 10.1117/12.300111

UNEP (2008) UN guide to climate neutrality-CCC, United Nations Environment Program, Nairobi, Kenya

Wang KS, Shih MH (2005) The thermal conductivity mechanism of sewage sludge ash lightweight material. *Cement and Concrete Research* 35(4):803-809, DOI: 10.1016/j.cemconres.2004.04.027

Yang T, Yao X, Zhang Z (2014) Geopolymer prepared with high-magnesium nickel slag: Characterization of properties and microstructure. *Construction and Building Materials* 59:188-194, DOI: 10.1016/j.conbuildmat.2014.01.038